Article

Folding of the Cerebral Cortex Requires Cdk5 in Upper-Layer Neurons in Gyrencephalic Mammals

Graphical Abstract
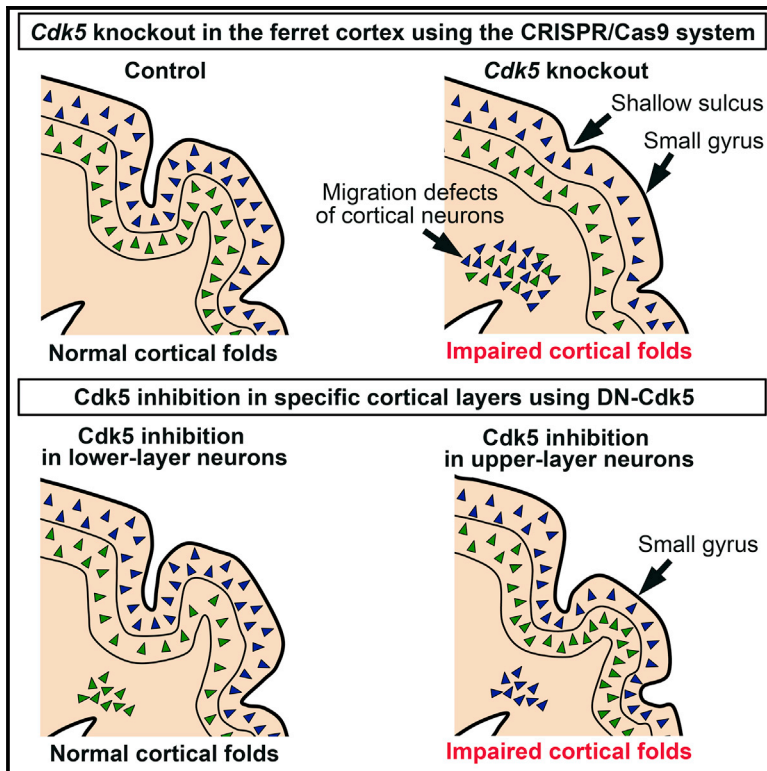
Authors
Yohei Shinmyo, Yukari Terashita,
Tung Anh Dinh Duong, ...,
Kazuyoshi Hosomichi, Atsushi Tajima,
Hiroshi Kawasaki

Correspondence
hiroshi-kawasaki@umin.ac.jp

In Brief
Shinmyo et al. describe a highly efficient gene knockout method for the folded cerebral cortex of ferrets using the CRISPR/Cas9 system. Loss-of-function studies of the *Cdk5* gene suggest that appropriate positioning of upper-layer neurons is crucial for cortical folding.

Highlights

- Efficient gene knockout in the ferret cerebral cortex was achieved using CRISPR/Cas9

- *Cdk5* knockout in the ferret cerebral cortex markedly impairs cortical folding

- Appropriate positioning of upper-layer neurons is critical for cortical folding

CellPress

OPEN
ACCESS
CellPress

Folding of the Cerebral Cortex Requires Cdk5 in Upper-Layer Neurons in Gyrencephalic Mammals

Yohei Shinmyo,[1,4] Yukari Terashita,[1,4] Tung Anh Dinh Duong,[1] Toshihide Horiike,[1] Muneo Kawasumi,[1] Kazuyoshi Hosomichi,[2] Atsushi Tajima,[2] and Hiroshi Kawasaki[1,3,5,*]

[1]Department of Medical Neuroscience, Graduate School of Medical Sciences, Kanazawa University, Ishikawa 920-8640, Japan
[2]Department of Bioinformatics and Genomics, Graduate School of Advanced Preventive Medical Sciences, Kanazawa University, Ishikawa 920-8640, Japan
[3]Brain/Liver Interface Medicine Research Center, Kanazawa University, Ishikawa 920-8640, Japan
[4]These authors contributed equally
[5]Lead Contact
*Correspondence: hiroshi-kawasaki@umin.ac.jp
http://dx.doi.org/10.1016/j.celrep.2017.08.024

SUMMARY

Folds in the cerebral cortex in mammals are believed to be key structures for accommodating increased cortical neurons in the cranial cavity. However, the mechanisms underlying cortical folding remain largely unknown, mainly because genetic manipulations for the gyrencephalic brain have been unavailable. By combining in utero electroporation and the CRISPR/Cas9 system, we succeeded in efficient gene knockout of *Cdk5*, which is mutated in some patients with classical lissencephaly, in the gyrencephalic brains of ferrets. We show that *Cdk5* knockout in the ferret cerebral cortex markedly impaired cortical folding. Furthermore, the results obtained from the introduction of dominant-negative Cdk5 into specific cortical layers suggest that Cdk5 function in upper-layer neurons is more important for cortical folding than that in lower-layer neurons. Cdk5 inhibition induced severe migration defects in cortical neurons. Taken together, our findings suggest that the appropriate positioning of upper-layer neurons is critical for cortical folding.

INTRODUCTION

Folding and expansion of the cerebral cortex during mammalian evolution are considered to be crucial advances in acquiring higher brain functions (Borrell and Götz, 2014; Fietz and Huttner, 2011; Kriegstein et al., 2006; Lui et al., 2011; Molnár et al., 2006; Poluch and Juliano, 2015; Rakic, 1995, 2009; Sun and Hevner, 2014; Zilles et al., 2013). The brains of humans, monkeys, and ferrets have the folded cerebral cortex (gyrencephalic cortex), whereas those of rodents often lack cortical folds (lissencephalic cortex). Furthermore, human patients with cortical folding malformations exhibit severe intellectual disability and epilepsy (Barkovich et al., 2012; Francis et al., 2006; Guerrini and Marini, 2006; Poduri et al., 2013). Therefore, molecular and cellular

mechanisms underlying formation and malformation of cortical folds have been of great interest (de Juan Romero et al., 2015; Fietz et al., 2010; Gertz and Kriegstein, 2015; Johnson et al., 2015; Masuda et al., 2015; Toda et al., 2016). However, our understanding of cortical folds is still rudimentary.

Candidate molecules responsible for cortical folding have been identified by pioneering studies of human disorders that exhibit anomalies in cortical folding, such as lissencephaly and polymicrogyria (Barkovich et al., 2012; Fry et al., 2014; Walsh, 1999). In classical lissencephaly (also known as type I lissencephaly), cortical folds are severely reduced or absent, and as a result, the surface of the brain becomes smooth. It has been assumed that several molecules which are mutated in some patients with classical lissencephaly such as *LIS1* (also known as *PAFAH1B1*), *doublecortin* (*DCX*), and *cyclin-dependent kinase 5* (*CDK5*) are involved in cortical folding (Kerjan and Gleeson, 2007; Magen et al., 2015; Pilz et al., 1998). However, it has not been experimentally tested if these genes really mediate cortical folding. Furthermore, the mechanistic links connecting these molecules and the macroscopic structures of folds have not yet been elucidated. It has been hypothesized that radial migration of neurons underlies folding of the cerebral cortex because a radial migration defect was found in *Cdk5* knockout mice (Gilmore et al., 1998; Ohshima et al., 2007). However, because the mouse brain does not have cortical folds, it has been difficult to determine the cellular mechanisms involved in cortical folding and the types of cells in which Cdk5 is responsible for cortical folding using mice.

Another reason why uncovering the mechanisms of cortical folding has been difficult to explore would be that rapid and efficient in vivo genetic manipulations that can be applied to the cerebral cortex of gyrencephalic mammals has been unavailable. To overcome this limitation, we recently established a genetic manipulation method for gyrencephalic carnivore ferrets to express genes of interest using in utero electroporation (IUE) (Kawasaki et al., 2012, 2013). Ferrets have well-developed brain structures and have been widely used for various neuroscientific research (Crowley and Katz, 2000; Fietz et al., 2010; Fujishiro et al., 2014; Huberman et al., 2005; Iwai et al., 2013; Kawasaki et al., 2004; Martínez-Martínez et al., 2016; Poluch and Juliano,
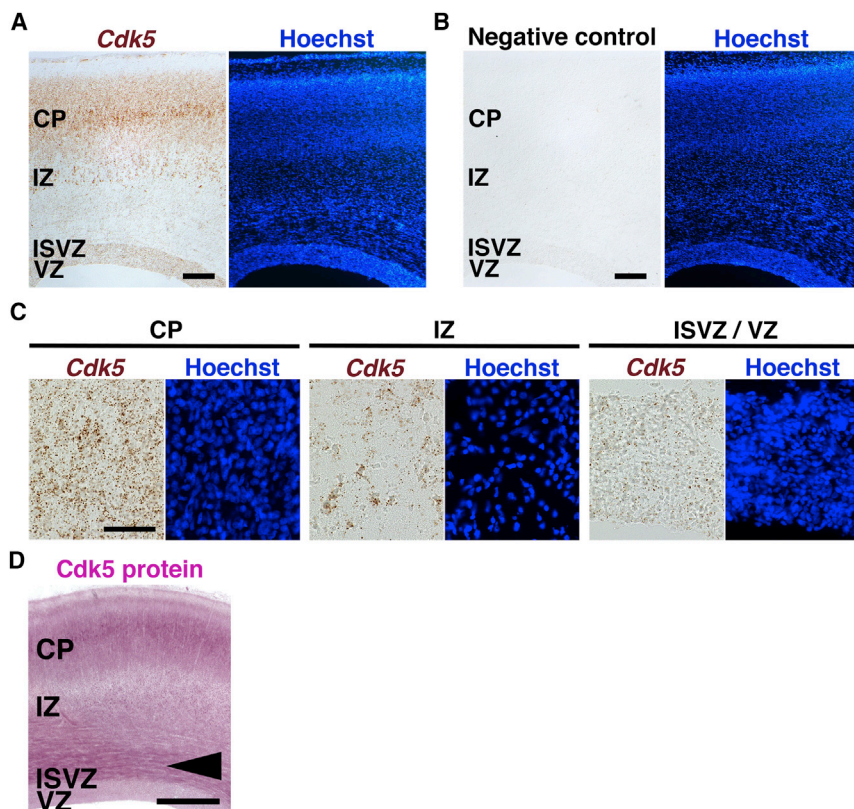
Figure 1. Expression Patterns of *Cdk5* mRNA and Its Protein in the Developing Ferret Brain

(A–C) RNAscope in situ hybridization was performed on coronal sections of ferret brains at P6 with a *Cdk5* probe (A and C) or a negative-control probe targeting the bacterial *dapB* gene (B). The sections were then stained with Hoechst 33342. (C) Higher magnification images of *Cdk5* expression in the cortical plate (CP), the intermediate zone (IZ), and the inner subventricular zone/ventricular zone (ISVZ/VZ). (A and C) *Cdk5* mRNA was expressed strongly in the CP of the ferret cerebral cortex. (B) No signal was detected when the negative-control probe was used. Scale bars, 500 μm (A and B) and 50 μm (C).

(D) Cdk5 immunohistochemistry using coronal sections of ferret brains at P6. As in the case of *Cdk5* mRNA, Cdk5 protein was most abundant in the CP of the cerebral cortex. Cdk5 immunoreactivity was also observed in axonal pathways in the cerebral cortex including the inner fiber layer (IFL) (arrowhead). Scale bar, 500 μm.

2015; Ware et al., 1999; White et al., 1999). Using our IUE method for ferrets, we recently demonstrated direct evidence for the role of subventricular zone (SVZ) progenitors in cortical folding (Toda et al., 2016). We further produced a ferret model of polymicrogyria by expressing fibroblast growth factor 8 (FGF8) and investigated the pathogenesis of polymicrogyria (Masuda et al., 2015). We decided that our next endeavor would be gene knockout in the ferret cerebral cortex. Because we recently reported that gene knockout was efficiently achieved in the mouse cerebral cortex by combining IUE and the CRIPSR/Cas9 system (Shinmyo et al., 2016), we tried to combine our IUE technique and the CRISPR/Cas9 system in ferrets. We found that this combination resulted in efficient gene knockout in the ferret cerebral cortex in vivo. By taking advantage of our gene knockout method for ferrets, we successfully found that Cdk5 in cortical neurons is indeed required for cortical folding. Furthermore, we found that the inhibition of Cdk5 in layer 2/3 reduced cortical folding, while that in layer 4 or layer 5/6 did not. These results suggest that upper-layer neurons are more critical than lower-layer neurons for cortical folding. Our findings provide mechanistic insights into cortical folding.

RESULTS

Expression Patterns of Cdk5 in the Developing Ferret Brain

We first examined the expression pattern of *Cdk5* mRNA in the ferret cerebral cortex at postnatal day 6 (P6). RNAscope in situ hybridization revealed that *Cdk5* mRNA was expressed preferentially in the cortical plate (CP), where the majority of postmitotic neurons accumulate (Figures 1A–1C). *Cdk5* mRNA was also expressed in the intermediate zone (IZ), which contains migrating neurons, and was weakly expressed in the ventricular zone (VZ) and inner subventricular zone (ISVZ) (Figures 1A and 1C). Consistently, when in situ hybridization with two distinct digoxigenin-labeled RNA probes was performed, *Cdk5* mRNA expression was observed predominantly in the CP (Figures S1A and S1B). We next examined the expression pattern of Cdk5 protein in the ferret cerebral cortex using anti-Cdk5 antibody. Consistent with *Cdk5* mRNA, Cdk5 protein was most abundant in the CP (Figure 1D), indicating that Cdk5 is expressed in cortical neurons in the ferret brain. Cdk5 immunoreactivity was also detected in axonal pathways in the cerebral cortex including the corpus callosum (Figure S1C) and the inner fiber layer (IFL) (Figure 1D, arrowhead). This result is consistent with previous studies demonstrating that Cdk5 protein was also found in the axons (Tsai et al., 1993) and our previous report that the axons in the IFL are derived, at least partially, from cortical neurons in ferrets (Kawasaki et al., 2013). Taken together with a previous report showing that Cdk5 is expressed in cortical neurons in mice (Tsai et al., 1993), these results indicate that the expression pattern of Cdk5 in the developing cerebral cortex is highly conserved between mice and ferrets. In addition, our immunostaining also showed that the expression pattern of Cdk5 protein was similar to that of *Cdk5* mRNA in the hippocampus and the thalamus (Figures S1D and S1E), suggesting that the anti-Cdk5 antibody used in this study specifically recognizes Cdk5 protein. This is also supported by the fact that Cdk5 immunoreactivity detected with this antibody was strongly reduced in the cerebral cortex of ferrets in which the *Cdk5* gene was knocked out by the CRISPR/Cas9 system (see below for details) (Figures 2A and 2B).
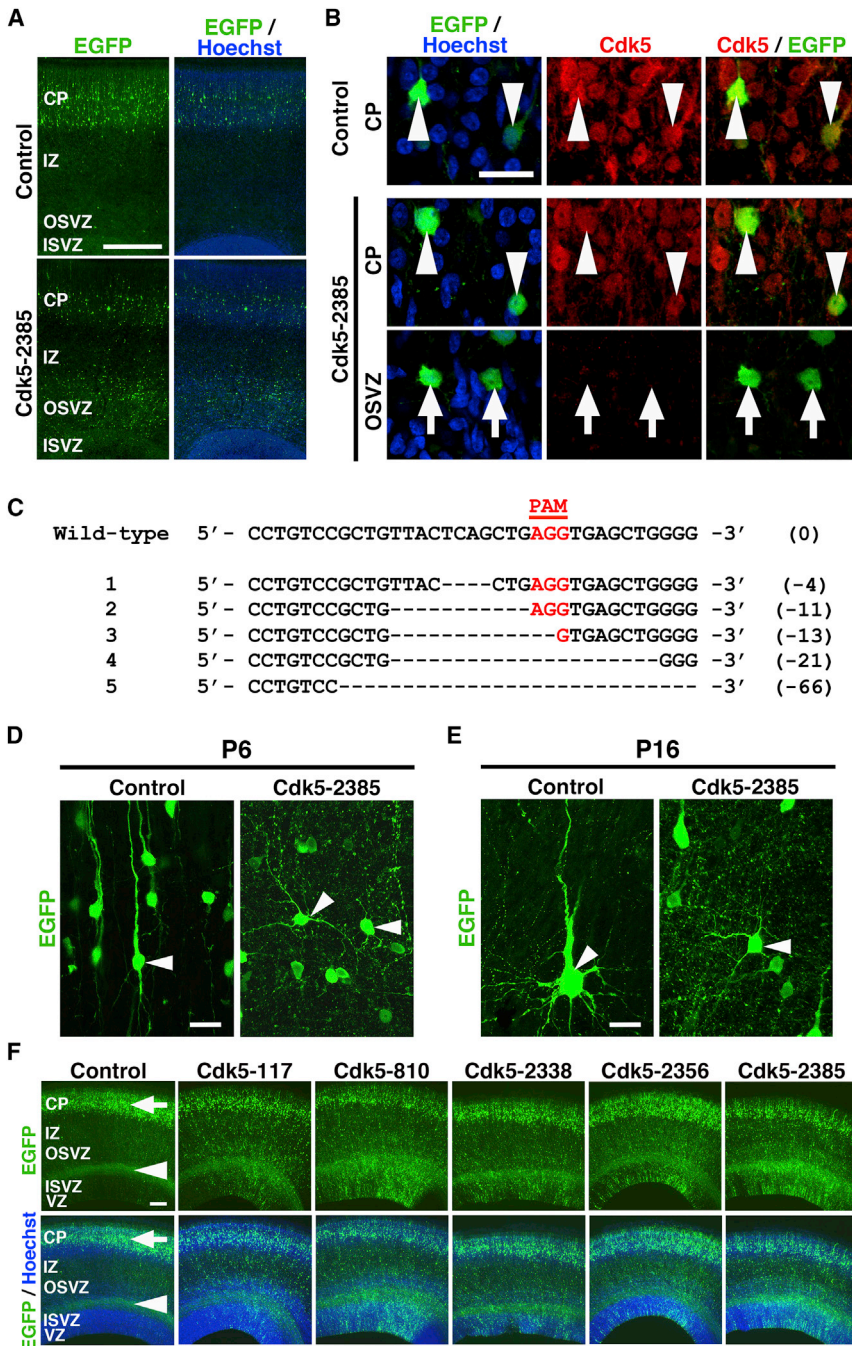
Figure 2. CRISPR/Cas9-Mediated Knockout of the *Cdk5* Gene in the Ferret Cerebral Cortex

(A and B) pCAG-EGFP plus either pX330-Cdk5 or control pX330 vector were introduced into the ferret cerebral cortex by using IUE at E31. Coronal sections were prepared at P6 and stained with anti-Cdk5 antibody and Hoechst 33342. (A) Note that many EGFP-positive cells remained accumulated in the outer subventricular zone (OSVZ) of the pX330-Cdk5-2385-electroporated cortex (lower panels). (B) Higher magnification confocal microscopic images of EGFP-positive cells in the CP and the OSVZ. Cdk5 expression was observed in EGFP-positive cells in the CP of the control brain (upper panels, arrowheads). Note that Cdk5 expression was greatly suppressed in EGFP-positive cells in the OSVZ of the pX330-Cdk5-2385-electroporated cortex (lower panels, arrows), while it was not strongly affected in the CP (middle panels, arrowheads). Scale bars, 500 μm (A) and 20 μm (B).

(C) Mutations found in the *Cdk5* locus. The wild-type sequence of the *Cdk5* gene and identified mutations are shown. The PAM sequence is marked in red. Dashes indicate deletions. The numbers in parentheses indicate the number of bases that had been changed.

(D and E) pCAG-EGFP plus either pX330-Cdk5-2385 or control pX330 vector were introduced into the ferret cerebral cortex by using IUE at E31. Coronal sections were prepared at P6 (D) and P16 (E) and stained with anti-GFP antibody. Arrowheads indicate representative images of EGFP-positive cells in the CP of the control cortex (left) and in the OSVZ of the pX330-Cdk5-2385-electroporated cortex (right). Note that the morphologies of EGFP-positive cells were markedly impaired by pX330-Cdk5-2385 at both P6 and P16. Scale bars, 20 μm.

(F) pCAG-EGFP plus either pX330-Cdk5 or control pX330 vector were introduced into the ferret cerebral cortex by using IUE at E31. Coronal sections were prepared at E39 and stained with Hoechst 33342. Note that all five pX330-Cdk5 constructs inhibited radial migration of EGFP-positive cells. Arrows and arrowheads indicate EGFP-positive neurons in the CP and EGFP-positive axons in the inner fiber layer, respectively. VZ, ventricular zone. Scale bar, 200 μm.

CRISPR/Cas9-Mediated Knockout of the *Cdk5* Gene in the Ferret Cerebral Cortex

We recently found that genes of interest could be knocked out with high efficiency in the developing cerebral cortex by combining the CRISPR/Cas9 system and IUE in mice (Shinmyo et al., 2016). This result raised the possibility that gene knockout can also be achieved in the cerebral cortex of ferrets. We therefore tried knockout of the *Cdk5* gene in the developing ferret cerebral cortex using our method. We chose five target sites in

the *Cdk5* gene: *Cdk5*-117 in exon 1; *Cdk5*-810 in exon 2; and *Cdk5*-2338, *Cdk5*-2356, and *Cdk5*-2385 in exon 7. We cloned these five target sequences in the pX330 plasmid, in which humanized Cas9 and synthetic chimeric guide RNA (sgRNA) are simultaneously expressed under the chicken β-actin hybrid and human U6 promoters, respectively (Cong et al., 2013). To evaluate the effectiveness of this gene knockout method in the cerebral cortex of ferrets, we first co-transfected pCAG-EGFP and pX330-Cdk5-2385 targeting a region near the serine 159, which is important for Cdk5 activation (Sharma et al., 1999), into the ferret cerebral cortex using IUE at E31

and prepared coronal sections at P6. Consistent with previous reports that Cdk5 is required for radial migration of cortical neurons in mice (Gilmore et al., 1998; Ohshima et al., 2007), radial migration of EGFP-positive cells was markedly inhibited in the pX330-Cdk5-2385-electroporated ferret cortex (Figure 2A, lower panels), while almost all EGFP-positive cells migrated into the CP in the control pX330-electroporated cortex (Figure 2A, upper panels). We next examined the expression of Cdk5 protein in EGFP-positive cells using immunohistochemistry. We found that Cdk5 expression was greatly suppressed in EGFP-positive cells in the outer subventricular zone (OSVZ) of the pX330-Cdk5-2385-electroporated cortex (Figure 2B, lower panels, arrows) compared with that in control pX330-electroporated cortex (Figure 2B, upper panels, arrowheads). A quantitative analysis revealed that Cdk5 expression was lost in 49% of EGFP-positive cells in the pX330-Cdk5-2385-electroporated cortex (control, $1.7\% \pm 1.7\%$; Cdk5-2385, $48.7\% \pm 5.9\%$; $p < 0.01$; Welch's t test, n = 3 animals for each condition). These results indicate that introduction of pX330-Cdk5-2385 using IUE efficiently knocked out the *Cdk5* gene in the ferret cerebral cortex.

To investigate the mutations caused by pX330-Cdk5-2385, we introduced pCAG-EGFP and pX330-Cdk5-2385 into the developing ferret cortex using IUE at E31. We then extracted genomic DNA from EGFP-positive areas of the cerebral cortex at P0. The target site of the *Cdk5* gene was amplified with PCR and sequenced using a next-generation sequencer. We found several kinds of deletion mutations near the predicted cleavage site in the *Cdk5* gene (Figure 2C). This result suggests that introduction of pX330-Cdk5-2385 induces insertion and deletion (indel) mutations in the *Cdk5* gene, leading to disruption of endogenous Cdk5 function.

It has been demonstrated that Cdk5 is required not only for radial migration of cortical neurons but also for multipolar-to-bipolar transition during radial migration in the mouse cerebral cortex (Gilmore et al., 1998; Ohshima et al., 2007). Therefore, we examined the position and the morphology of the EGFP-positive cells in the ferret cortex at P6 and P16. In the control pX330-electroporated cortex at P6, most EGFP-positive neurons migrated into the CP and had a bipolar morphology with one major leading process oriented toward the cortical surface (Figures 2D and S2A, control). In contrast, many EGFP-positive cells in the pX330-Cdk5-2385-electroporated cortex exhibited radial migration defects and abnormal morphologies with multiple processes (Figures 2D and S2A, Cdk5-2385), suggesting that multipolar-bipolar transition is inhibited by pX330-Cdk5-2385. Similar results were also obtained at P16. While EGFP-positive cells in lower layers of the CP exhibited developed dendritic arbors in the control cortex (Figures 2E and S2B, control), EGFP-positive cells in the pX330-Cdk5-2385-electroporated cortex were still positioned within the IZ and the SVZ and kept their multipolar morphology (Figures 2E and S2B, Cdk5-2385). These results suggest that IUE of pX330-Cdk5-2385 efficiently disrupts the *Cdk5* genome in the ferret cerebral cortex.

Because we made five kinds of pX330-Cdk5 constructs, we compared their effectiveness for disrupting Cdk5 function. We co-transfected pCAG-EGFP and one of the pX330-Cdk5 constructs into the ferret cerebral cortex using IUE at E31. We then prepared coronal sections at E39 and examined the distribution of EGFP-positive cells. In the control brain, which was electroporated with the pX330 plasmid and pCAG-EGFP, EGFP-positive cells were normally distributed in the CP (Figure 2F, control, arrows). In addition, EGFP-positive axons were observed between the OSVZ and the ISVZ (Figure 2F, control, arrowheads). In contrast, when pX330-Cdk5-117, pX330-Cdk5-810, pX330-Cdk5-2338, pX330-Cdk5-2356, or pX330-Cdk5-2385 were electroporated, radial migration of EGFP-positive cells was inhibited, and many EGFP-positive cells remained accumulated in the IZ and the SVZ (Figure 2F), suggesting that the *Cdk5* gene is disrupted by all of the pX330-Cdk5 constructs. In the following experiments, we mainly used the pX330-Cdk5-2385 construct to knock out the *Cdk5* gene because pX330-Cdk5-2385 seemed to inhibit the radial migration of EGFP-positive cells most effectively. Taken together, our data indicate that combining our IUE for ferrets and the CRISPR/Cas9 system should be useful for investigating gene functions in higher mammals by knocking out genes of interest.

Reduced Cortical Folding in the pX330-Cdk5-2385-Electroporated Brain

A previous report found a mutation in the *CDK5* gene in human patients with lissencephaly (Magen et al., 2015). Because Cdk5 is abundantly expressed in cortical neurons, it has been proposed that Cdk5 in cortical neurons is required for cortical folding. To directly test whether Cdk5 in cortical neurons is indeed essential for cortical folding, we introduced pCAG-EGFP and pX330-Cdk5-2385 into the ferret cerebral cortex using IUE at E31, and the brains were prepared at P16, when cortical folds have already been formed. Interestingly, we found clear abnormalities in cortical folding of the EGFP-positive area of the pX330-Cdk5-2385-electroporated cortex (Figures 3A and 3B, squares in lower panels), while no apparent abnormalities were observed in the control cortex electroporated with the pX330 plasmid (Figures 3A and 3B, upper panels).

Hoechst staining of coronal sections revealed that the pX330-Cdk5-2385-electroporated cortex had the following two characteristics in abnormal cortical folding. First, the size of the gyrus in the pX330-Cdk5-2385-transfected cortex was remarkably smaller than that in the contralateral non-transfected side (Figures 3C and 3D; compare iii and iv, arrowheads). Second, the depth of the sulcus in the pX330-Cdk5-2385-transfected cortex was markedly shallower than that in the contralateral non-transfected side (Figures 3C and 3D; compare iii and iv, arrows).

It was shown that a multiple-target CRISPR strategy, in which multiple kinds of sgRNAs targeting the same gene were used, was an efficient approach to induce biallelic mutations in the target gene (Sunagawa et al., 2016). Thus, we introduced a mixture of three kinds of pX330-Cdk5 constructs (pX330-Cdk5-810, pX330-Cdk5-2356, and pX330-Cdk5-2385) into the ferret cerebral cortex using IUE. We found that the cortex transfected with these pX330-Cdk5 constructs showed impaired cortical folding, which was similar to that in the pX330-Cdk5-2385-transfected cortex (see Figures 3E–3G for details).

We quantified the size of the gyrus on the electroporated side and the contralateral side of brain sections (Figure S3A). To minimize the variation of the size of the gyrus depending on the position of coronal sections along the anterior-posterior axis,
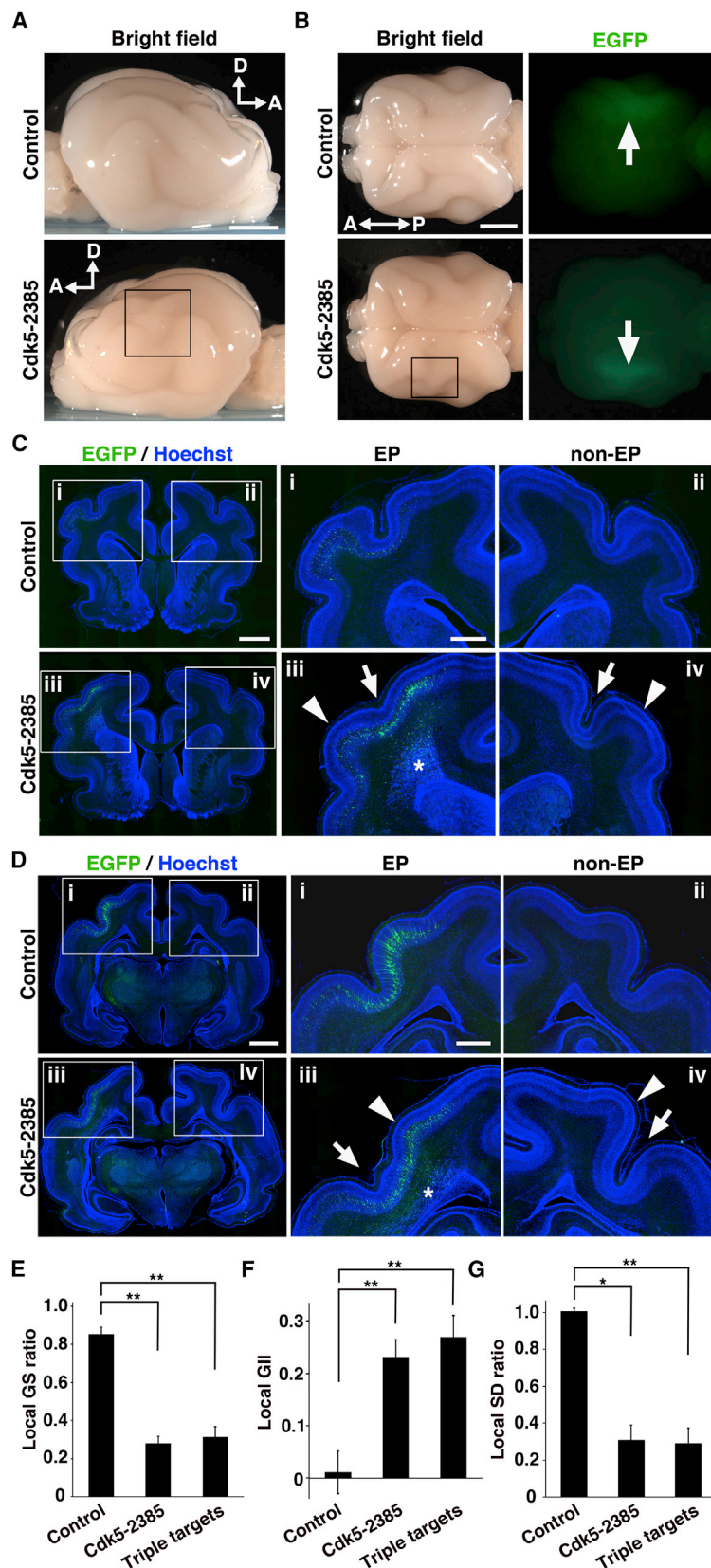
Figure 3. Cdk5 in the Developing Ferret Cortex Is Required for Cortical Folding

(A and B) Lateral (A) and dorsal (B) views of electroporated brains at P16. pCAG-EGFP plus either pX330-Cdk5-2385 or control pX330 vector were introduced into the cerebral cortex of ferret brains by using IUE at E31, and the brains were prepared at P16. Electroporated areas showed EGFP fluorescence (B, arrows). Cortical folding was impaired in animals transfected with pX330-Cdk5-2385 (squares). A, anterior; D, dorsal; P, posterior. Scale bars, 4 mm.

(C and D) Coronal sections of the electroporated brains were stained with Hoechst 33342. The areas within the boxes in the left panels are magnified and shown in the right panels. Note marked reductions in the depth of the sulcus (arrows) and in the size of the gyrus (arrowheads) on the pX330-Cdk5-2385-electroporated side of the cortex compared with the non-electroporated side of the cortex and the cortex in control animals. The asterisks indicate an ectopic cell population in the white matter. EP, electroporated side; non-EP, non-electroporated side. Scale bars, 2 mm (left panels) and 1 mm (middle panels).

(E–G) Quantification of the local GS ratio (E), the local GII (F), and the local SD ratio (G). See also Figure S3 for details. pCAG-EGFP plus either pX330-Cdk5-2385 (5 mg/mL), a mixture of three pX330-Cdk5 constructs (triple targets, 1.67 mg/mL each), or control pX330 vector (5 mg/mL) was introduced using IUE at E31, and the brains were prepared at P16. The local GS (E) and the local SD (G) ratios were significantly reduced in the cortices transfected with pX330-Cdk5-2385 or three pX330-Cdk5 constructs. The local GII value (F) was significantly larger in these brains (n = 4 animals for control and triple targets, and n = 3 for Cdk5-2385; **p < 0.01; *p < 0.05; Welch's t test, two-tailed). Bars represent mean ± SEM.

the value for the size of the gyrus on the electroporated side was divided by that on the contralateral side to give the local gyrus size ratio (local GS ratio). The local GS ratio would be 1 if the size of the gyrus was the same between the electroporated side and the other side and would be zero if gyrus formation was completely blocked by genetic manipulation. Consistent with our observations, we found that the local GS ratio was significantly smaller in the cortices transfected with pX330-Cdk5-2385 or a mixture of three pX330-Cdk5 constructs (triple targets) than in the control cortex (control, 0.85 ± 0.038; Cdk5-2385, 0.28 ± 0.036; triple targets, 0.31 ± 0.055; **p < 0.01; Welch's t test) (Figure 3E).

To quantify the degree of inhibition of cortical folding, the length of the complete inner contour was divided by that of the outer contour of the cortex between two gyri in EGFP-positive cortical areas (Figure S3B, local GI). We then defined the local gyrification inhibition index (local GII) in which the local GI value on the contralateral side was subtracted by that on the electroporated side and then divided by that on the contralateral side (Figure S3B). The local GII value would be zero if cortical folds were same between the transfected side and the other side and would be larger than zero if cortical folds were suppressed by genetic manipulation. We found that the local GII value was significantly larger in the cortices transfected with pX330-Cdk5-2385 or three pX330-Cdk5 constructs than in the control cortex (control, 0.011 ± 0.041; Cdk5-2385, 0.23 ± 0.034; triple targets, 0.27 ± 0.042; **p < 0.01; Welch's t test) (Figure 3F).

Furthermore, we defined another index, the local sulcus depth index (local SD), which represents the depth of the sulcus (Figure S3C). The local SD ratio would be 1 if the depth of the sulcus was the same between the electroporated side and the other side and would be zero if sulcus formation was totally blocked by genetic manipulation. The local SD ratio in the cortices transfected with pX330-Cdk5-2385 or three pX330-Cdk5 constructs was significantly smaller than that in the control cortex (control, 1.00 ± 0.019; Cdk5-2385, 0.31 ± 0.084; triple targets, 0.29 ± 0.086; *p < 0.05, **p < 0.01; Welch's t test) (Figure 3G). Taken together, these results clearly indicate that cortical folding is inhibited in the pX330-Cdk5-2385-electroporated cortex. Our findings also indicate that Cdk5 in cortical neurons is indeed required for cortical folding.

The pX330-Cdk5-2385-Electroporated Cortex Showed Radial Migration Deficits of Cortical Neurons

It has been hypothesized that the impaired cortical folding in human lissencephaly is caused by radial migration deficits of cortical neurons (Kerjan and Gleeson, 2007). Consistent with this hypothesis, in the pX330-Cdk5-2385-electroporated cortex, we observed an ectopic cell population in the white matter beneath reduced cortical folding (Figures 3C, 3D, and 4A, asterisks). Immunostaining with anti-NeuN antibody, which recognizes post-mitotic neurons, showed that many cells in this cell population were positive for NeuN (Figure 4B), suggesting that radial migration of cortical neurons was impaired massively. In contrast, immunostaining for the glial markers glial fibrillary acidic protein (GFAP), glutamine synthetase (GS), adenomatous polyposis coli (APC), and Olig2 showed that glial cells were not accumulated in this cell population (Figures 4C and S4A–S4D).

These results suggest that when the Cdk5 gene is knocked out, the defect in radial migration of cortical neurons results in impaired cortical folding in the ferret cortex.

Next, we investigated subtypes of cortical neurons showing radial migration defects. Our previous studies showed that when IUE was performed at E31, EGFP-positive neurons were preferentially located in layer 5/6 (Kawasaki et al., 2012). Indeed, when pCAG-EGFP and pX330 control plasmid were introduced at E31, EGFP-positive neurons were predominantly localized in layer 5/6, which is Ctip2- and FoxP2-positive (Figure 4D), rather than in layers 2–4, which are Cux1- and Rorb-positive. Interestingly, although the ectopic cell population in the white matter of the pX330-Cdk5-2385-electroporated cortex contained EGFP-positive cells, there were not very many EGFP-positive cells (Figure 4E). The proportion of EGFP-positive cells among NeuN-positive cells in the ectopic cell population was 15.5% ± 1.9% (n = 3 brains). To examine whether radial migration of upper-layer neurons was inhibited, we performed in situ hybridization for Cux1 and Rorb, which are expressed in layers 2–4 and layer 4, respectively (Figure 4F). We found that many cells in the ectopic cell population expressed Cux1 rather than Rorb (Figure 4G). These results suggest that although the pX330-Cdk5-2385-electroporated cortex showed radial migration deficits of both upper-layer and lower-layer neurons, radial migration of upper-layer neurons seemed to be preferentially impaired in the pX330-Cdk5-2385-electroporated cortex.

Inhibition of Cdk5 Function in Layer 2/3 Impaired Cortical Folding

Because introduction of pX330-Cdk5-2385 using IUE at E31 disrupted the Cdk5 gene in most layers of the cerebral cortex, it was unclear which neurons' radial migration was important for cortical folding. Our findings that the radial migration of upper-layer neurons was more severely impaired by pX330-Cdk5-2385 raised the possibility that upper-layer neurons are more critical than lower-layer neurons for cortical folding. To test this possibility, we blocked Cdk5 function in distinct populations of cortical neurons by introducing dominant-negative Cdk5 (DN-Cdk5) using IUE at E31, E34, and E37 (Borrell, 2010; Kawauchi et al., 2003; Ohshima et al., 2007). To make DN-Cdk5, Asp at codon 144 of the Cdk5 protein was replaced with Asn, and as a result, the kinase activity of Cdk5 was lost. This DN-Cdk5 has been characterized in many papers and has been widely used. It is well-known that this DN-Cdk5 suppresses the function of endogenous Cdk5 (Kawauchi et al., 2003, 2006; Ohshima et al., 2007).

First, we examined the distribution of EGFP-positive cells in the control cortex electroporated with pCAG-EGFP and pCAG vector (control plasmid for pCAG-DN-Cdk5). Consistent with our previous results (Kawasaki et al., 2012), we observed EGFP-positive cells in layers 5/6 and 2/3 in the control brain electroporated at E31 and E37, respectively (Figure S5A, upper and lower panels). In addition, IUE at E34 preferentially induced the EGFP expression in layer 4 neurons (Figure S5A, middle panels). It has been shown that glial cells are generated after upper-layer neurons are produced in mice (Kriegstein and Alvarez-Buylla, 2009). To examine whether IUE at E37 resulted in the transgene expression in glial cells in ferrets in addition to layer 2/3 neurons,
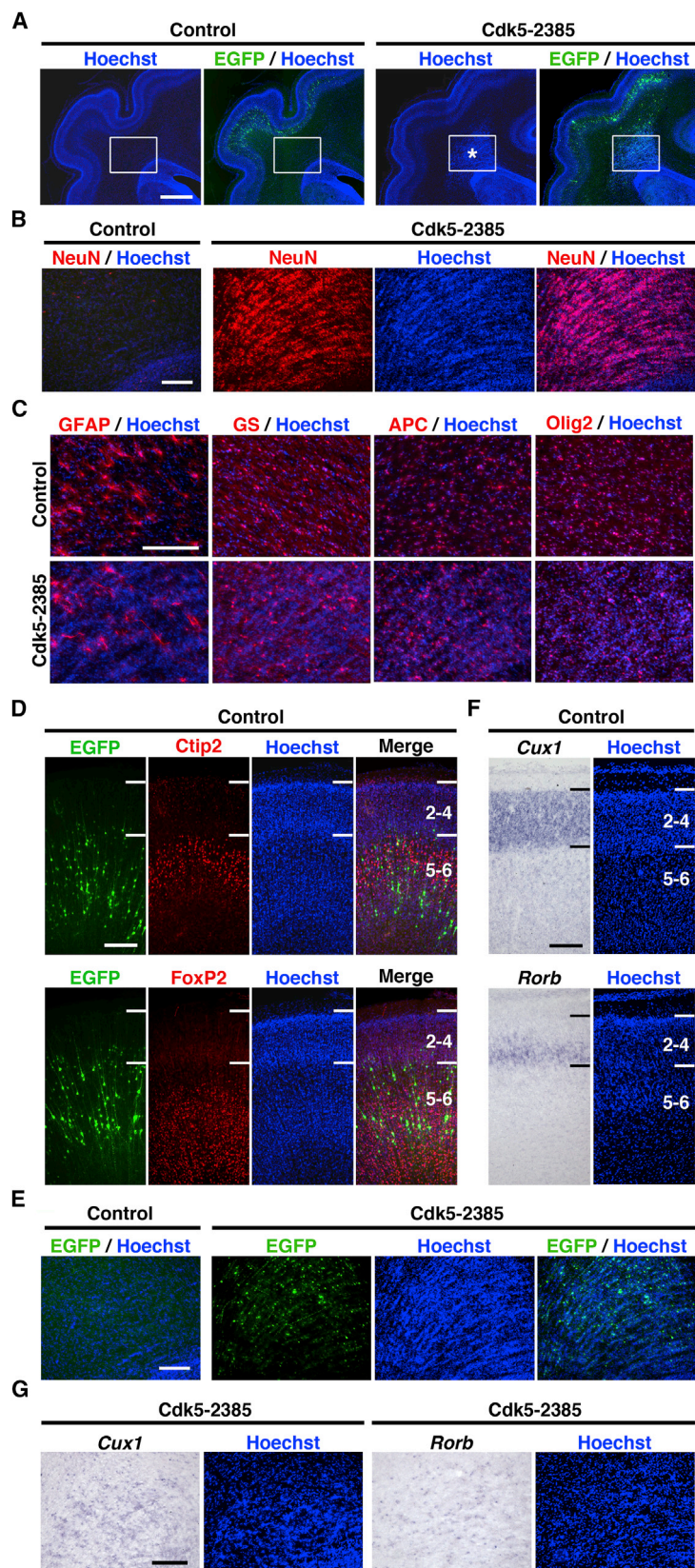
Figure 4. Radial Migration of Cortical Neurons Was Impaired in the pX330-Cdk5-2385-Electroporated Cortex

pCAG-EGFP plus either pX330-Cdk5-2385 or control pX330 vector were introduced into the cerebral cortex of ferret brains by using IUE at E31, and the brains were prepared at P16.

(A and B) Coronal sections of the electroporated brains were stained with Hoechst 33342 and anti-NeuN antibody. The areas within the boxes in (A) are magnified and shown in (B). Note that many cells in the ectopic cell population (A, asterisk) were positive for NeuN. Scale bars, 1 mm in (A) and 200 μm in (B).

(C) Coronal sections of the electroporated brains were stained with Hoechst 33342 plus either anti-GFAP, anti-GS, anti-APC, or anti-Olig2 antibody. Note that glial cells were not abnormally accumulated in the ectopic cell population. Scale bar, 200 μm.

(D) Coronal sections of the control EGFP-electroporated brains were stained with Hoechst 33342 plus either anti-Ctip2 antibody or anti-FOXP2 antibody. Note that EGFP-positive cells were preferentially observed in layer 5/6. Numbers indicate layers in the cortex. Scale bar, 200 μm.

(E) Coronal sections of the electroporated brains were stained with Hoechst 33342. Note that the ectopic cell population was composed of EGFP-positive and EGFP-negative cells. Scale bar, 200 μm.

(F) *Cux1* and *Rorb* expression in the control ferret cortex. Hoechst 33342 staining and in situ hybridization for *Cux1* or *Rorb* were performed using coronal sections of the cerebral cortex at P16. *Cux1* mRNA was enriched in layers 2–4, whereas *Rorb* mRNA selectively labeled layer 4. Scale bar, 200 μm.

(G) *Cux1* and *Rorb* expression in the ectopic cell population of the pX330-Cdk5-2385-transfected cortex. Hoechst 33342 staining and in situ hybridization for *Cux1* or *Rorb* were performed in coronal sections of the pX330-Cdk5-2385-electroporated brains. Note that *Cux1* mRNA was abundantly expressed in the ectopic cell population. Scale bar, 200 μm.

we examined the expression of APC and GS. Our confocal microscopic analysis revealed that all EGFP-positive cells were positive for NeuN (Figure S5B, arrowheads), but negative for APC and GS (Figure S5B, arrows). These results indicate that IUE at E37 led to selective transgene expression in neuronal cells in ferrets. Thus, IUE at E31, E34, and E37 enabled selective transgene expression in layer 5/6, layer 4, and layer 2/3 cortical neurons, respectively.

When we co-transfected EGFP and DN-Cdk5 into the ferret cortex using IUE, we found that the vast majority of EGFP-positive cells were located in the IZ and SVZ (Figures 5A for E31, 5B for E34, 5C for E37, DN-Cdk5, asterisks, and S5C, lower panels, arrows). In contrast, most EGFP-positive cells migrated into the CP in the control cortex (Figures 5A–5C, control, and S5C, upper panels, arrowheads). These results indicate that Cdk5 is essential for radial migration of both upper-layer neurons and lower-layer neurons because IUE of DN-Cdk5 at E31, E34, and E37 impaired radial migration of EGFP-positive neurons. Detailed examination of cell morphology showed that DN-Cdk5 induced abnormal morphologies with multiple short processes at P16 (Figure S5D). These results are consistent with our findings from *Cdk5* knockout experiments using the CRISPR system (Figures 2 and 3). Next, we examined cortical folding of the DN-Cdk5-electroporated cortex. Interestingly, we found obvious defects in cortical folding when DN-Cdk5 was expressed at E37 (Figure 5C, DN-Cdk5, arrows). Importantly, the defects in cortical folding were observed in the area close to EGFP-positive transfected areas (Figure 5C, DN-Cdk5, arrows), but not near EGFP-positive areas in the control brain (Figure 5C, control, arrowheads). Interestingly, in contrast to IUE at E37, IUE at E31 or E34 did not affect cortical folding even when DN-Cdk5 was expressed (Figures 5A and 5B, DN-Cdk5, arrowheads). Consistently, we found that the local GS ratio was significantly smaller in the DN-Cdk5-transfected cortex than in the control cortex when IUE was performed at E37 (control, 1.00 ± 0.10; DN-Cdk5, 0.65 ± 0.12; p < 0.05; Welch's t test) (Figure 5D, right). In contrast, no significant differences of the local GS ratio between DN-Cdk5-transfected and control cortices were observed when IUE was performed at E31 or E34 (Figure 5D, left and middle). These results suggest that radial migration of layer 2/3 neurons is more critical than those of layers 4–6 neurons for cortical folding. In addition, it should be noted that we also measured the local GII and the local SD ratio, but did not find significant differences in all conditions (Figures S5E and S5F). This is presumably because the effect of DN-Cdk5 is weaker than that of *Cdk5* knockout by the CRISPR/Cas9 system, and the local GS ratio is most sensitive to changes in cortical folding.

Cell Proliferation and Apoptosis Were Not Affected in the pX330-Cdk5-2385-Transfected Cortex

Our findings suggest that radial migration defects of cortical neurons resulted in impaired cortical folding in the *Cdk5* knockout cortex (Figure 3). However, it remained possible that impaired cortical folding was caused by decreased cell proliferation and/or increased apoptosis. To test this possibility, we first immunostained for the proliferation markers Ki-67 and phospho-histone H3 (pHH3). We found that both Ki-67-positive (Figures S4E and S4F) and pHH3-positive (Figures S4G and S4H)

cells were not affected by pX330-Cdk5-2385. We also investigated neural progenitors by immunostaining for Pax6 and found that Pax6-positive neural progenitors were not affected in the pX330-Cdk5-2385-transfected cortex (Figures S4I and S4J). We next performed immunostaining with anti-cleaved caspase-3 antibody to detect apoptosis and found that cleaved caspase-3-positive cells were not increased by pX330-Cdk5-2385 (Figures S4K and S4L). Taken together, these results suggest that cell proliferation and apoptosis were not involved in the impaired cortical folding resulting from *Cdk5* knockout.

DISCUSSION

Here, we established a gene knockout method for the gyrencephalic brain by combining IUE for ferrets and the CRISPR/Cas9 system. Using our method, we clearly demonstrated the indispensable role of Cdk5 in cortical folding in the gyrencephalic brain of ferrets. Furthermore, our data suggest that normal radial migration of upper-layer neurons regulated by Cdk5 is essential for cortical folding.

Establishment of a Gene Knockout Method for the Cerebral Cortex of Gyrencephalic Mammals

The CRISPR/Cas9 system is widely used to generate gene knockout animals. In this study, we demonstrated efficient knockout of the *Cdk5* gene in the ferret cerebral cortex by combining the CRISPR/Cas9 system and our IUE method for ferrets. Our data showed that the pX330-Cdk5-2385-transfected cortex has more severe defects in cortical folding than the DN-Cdk5-transfected cortex (Figures 3 and 5), suggesting that pX330-Cdk5, compared to DN-Cdk5, inhibited Cdk5 function more severely and more massively. This result is presumably due to a difference in technical features between the two experimental systems (Figure S5G). When EGFP plasmids and DN-Cdk5 plasmids are co-transfected using IUE, Cdk5 functions are suppressed only in EGFP-positive neurons produced immediately after IUE and those in EGFP-negative descendant neurons produced after several rounds of cell division are not. This is because plasmids are not duplicated during cell division in neural progenitors.

In contrast, when the CRISPR/Cas9 construct pX330-Cdk5 and EGFP plasmids are co-transfected, pX330-Cdk5 disrupts the target genome in transfected cells, and all descendant neurons, including both EGFP-positive and EGFP-negative neurons, have the disrupted genome (Figure S5G). Therefore, it seems plausible that IUE of pX330-Cdk5-2385 at E31 disrupts the *Cdk5* gene in neural stem cells and/or progenitor cells, resulting in generation of both lower-layer neurons and upper-layer neurons lacking Cdk5 function. A similar phenomenon was observed in a previous report showing CRISPR/Cas9-mediated gene knockout in the mouse brain using IUE (Kalebic et al., 2016). Thus, our data indicate that the combination of the CRISPR/Cas9 system and IUE is a powerful and efficient approach to achieve gene knockout in the cerebral cortex of gyrencephalic mammals.

The Importance of Upper-Layer Neurons in Cortical Folding

Although a mutation was identified in the *CDK5* gene of human patients with classical lissencephaly (Magen et al., 2015), it
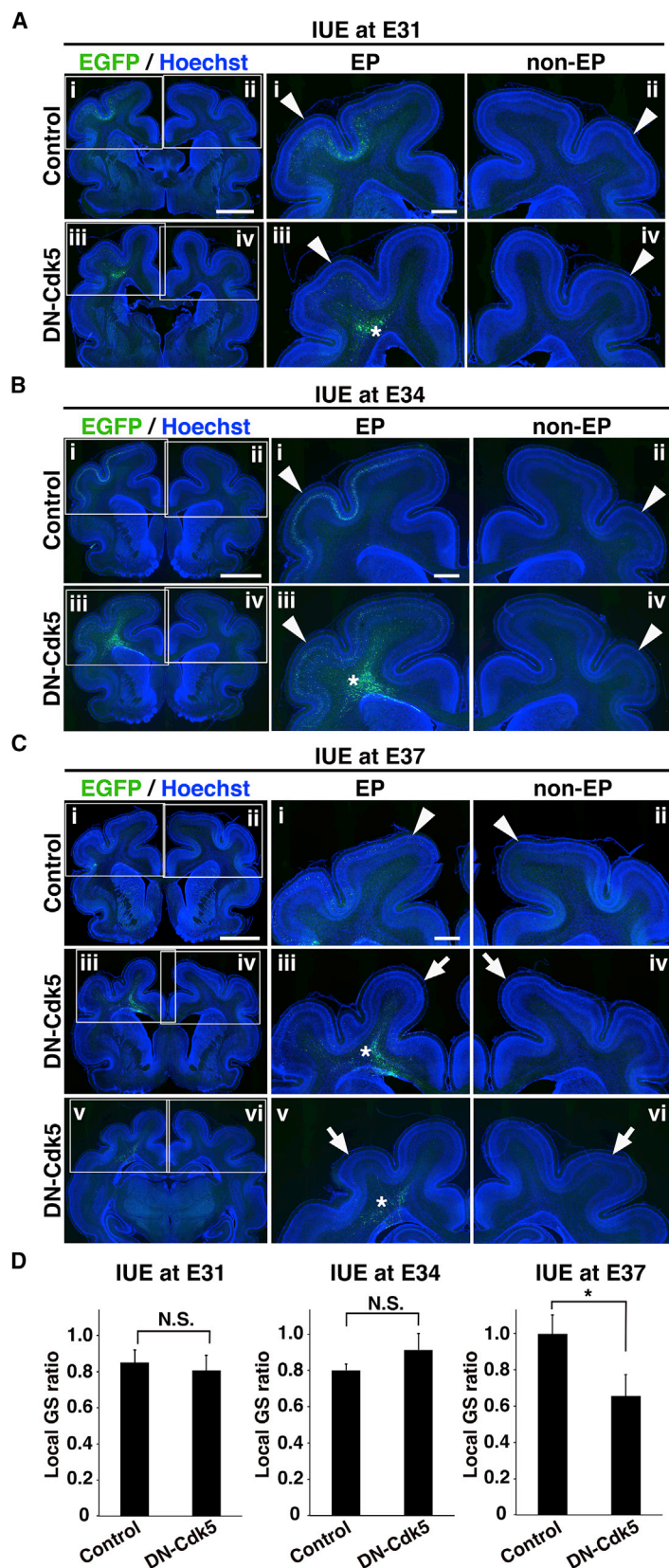
Figure 5. Cdk5 in Layer 2/3 Is Required for Cortical Folding in the Ferret Cortex

(A–C) pCAG-EGFP plus either pCAG-DN-Cdk5 or control pCAG vector were introduced into the cerebral cortex of ferret brains by using IUE at E31 (A), E34 (B), or E37 (C), and the brains were prepared at P16. Coronal sections of the electroporated brains were stained with Hoechst 33342. The areas within the boxes in the left panels are magnified and shown in the right panels. It should be noted that cortical folding was impaired in brains electroporated with DN-Cdk5 at E37 (C, arrows), but not E31 and E34 (A and B, arrowheads), although radial migration of EGFP-positive cells was impaired in all cases (asterisks). Scale bars, 3 mm (left panels) and 1 mm (middle panels). (D) Quantification of the local GS ratio. The local GS ratio was significantly reduced in brains electroporated with DN-Cdk5 at E37 (n = 3 and 4 animals for DN-Cdk5 and control samples, respectively), but not at E31 (n = 3 animals for each condition) and E34 (n = 3 animals for each condition). *p < 0.05; N.S., not significant. Welch's t test, one-tailed. Bars represent mean ± SEM.

had not been directly tested if *Cdk5* is involved in cortical folding experimentally. We demonstrated that *Cdk5* knockout in the ferret cerebral cortex markedly impaired radial migration of cortical neurons and cortical folding (Figures 3 and 4). This result suggests that Cdk5 is critical for cortical folding. Furthermore, our data using DN-Cdk5 suggests that radial migration of upper-layer neurons is more critical for cortical folding than that of lower-layer neurons (Figure 5). Thus, we propose that the appropriate positioning of upper-layer neurons is critical for cortical folding.

Although a number of hypotheses for the mechanisms of cortical folding have been proposed (Kriegstein et al., 2006; Lui et al., 2011; Zilles et al., 2013), the molecular and cellular mechanisms underlying cortical folding remain largely unknown. This is mainly because genetic manipulation techniques for gyrencephalic mammals had been missing. Using our recently developed genetic techniques for ferrets, we show the importance of upper-layer neurons in cortical folding. Because the ratio of the number of upper-layer neurons to that of lower-layer neurons is much greater in gyrencephalic humans than in lissencephalic rodents (DeFelipe et al., 2002), it has been hypothesized that expansion of upper layers in comparison to lower layers contributes to the development of cortical folds during evolution (Richman et al., 1975). This hypothesis is consistent with our model, which assumes that upper-layer neurons are more critical than lower-layer neurons for cortical folding. It seemed plausible that an expanded cortical surface produced by increased upper-layer neurons is essential for generating the protrusions of the cerebral cortex (i.e., gyri). This hypothesis is further supported by our previous studies using ferrets showing that upper layers are preferentially decreased in gyri, when cortical folding is impaired by Tbr2 inhibition (Toda et al., 2016). Furthermore, upper layers are preferentially increased in polymicrogyria induced by ectopic expression of FGF8 (Masuda et al., 2015). It should be noted that the pX330-Cdk5-2385-transfected cortex has more severe defects in cortical folding than the DN-Cdk5-transfected cortex (Figures 3 and 5). This is presumably because introduction of pX330-Cdk5, compared to DN-Cdk5, inhibited Cdk5 function in layer 2/3 neurons more extensively, but it remains possible that Cdk5 in lower-layer neurons also plays a role in cortical folding.

A Conserved Role of Cdk5 for Radial Migration of Cortical Neurons

Although the expression and functions of Cdk5 in the cerebral cortex have been investigated in mice (Ohshima et al., 2007; Tsai et al., 1993), those in higher mammals are largely unknown. Our study showed that *Cdk5* mRNA was predominantly expressed in the CP of the ferret cerebral cortex (Figures 1A–1C). Interestingly, Cdk5 protein was abundantly distributed in the IFL (Figure 1D), which is a prominent feature of the cerebral cortex in higher mammals (Smart et al., 2002; Zecevic et al., 2005). This result is consistent with previous studies demonstrating that Cdk5 protein was also found in the axons (Tsai et al., 1993) and our previous report that the axons in the IFL are derived, at least partially, from cortical neurons in ferrets (Kawasaki et al., 2013).

We demonstrated that Cdk5 is essential for radial migration of cortical neurons in the ferret cortex by two different loss-of-func-

tion approaches (Figures 2 and 5). In addition, our data suggest that Cdk5 is required for multipolar-to-bipolar transition during radial neuronal migration in ferrets (Figures 2D, 2E, and S5D). These are consistent with the results of *Cdk5* knockout experiments in mice (Ohshima et al., 2007). Furthermore, because aberrant organization of the cortical layers was observed in human patients with a loss-of-function mutation of *CDK5* gene (Magen et al., 2015), the function of Cdk5 in the cerebral cortex seems to be highly conserved across mammalian species.

A Ferret Model of Classical Lissencephaly

Animal models of human disease are essential for understanding the pathogenesis of diseases and exploring novel therapies. Because rodents do not have a gyrated cortex, it is impossible to create mouse models of human diseases which involve abnormal cortical folding such as classical lissencephaly. Classical lissencephaly is caused by mutations of the *LIS1* or *DCX* genes (Pilz et al., 1998). These genes encode microtubule-associated proteins that regulate cytoskeletal dynamics and are required for radial migration of cortical neurons (Pramparo et al., 2010; Wynshaw-Boris, 2007). Other genes that are associated with classical lissencephaly include *reelin* (*RELN*) and *very low density lipoprotein receptor* (*VLDLR*), which are also essential for radial migration of cortical neurons (Boycott et al., 2005; Hong et al., 2000). In this study, we showed that in the pX330-Cdk5-2385-transfected cortex, cortical neurons displayed deficits in radial migration and there was reduced cortical folding, which is reminiscent of classical lissencephaly. In addition, we found an ectopic cell population in the white matter, which is similar to the subcortical band heterotopia observed in classical lissencephaly (Barkovich et al., 2012). Therefore, our ferret model using pX330-Cdk-2385 enabled us to investigate the pathophysiological mechanisms of classical lissencephaly. Importantly, because it takes only a few weeks to make our ferret models, our technique combining IUE and the CRIPSR/Cas9 using ferrets could lead to uncovering the entire picture of the molecular mechanisms underlying cortical folding and move us closer to the ultimate goal of understanding the human brain and its diseases.

EXPERIMENTAL PROCEDURES

Animals
Normally pigmented, sable ferrets (*Mustela putorius furo*) were purchased from Marshall Farms (North Rose, NY). Ferrets were maintained as described previously (Iwai and Kawasaki, 2009; Iwai et al., 2013; Kawasaki et al., 2004). The day of conception was counted as embryonic day 0 (E0), and the day of birth was designated as postnatal day 0 (P0). All procedures were performed in accordance with protocols approved by the Animal Care Committee of Kanazawa University.

IUE for Ferrets
IUE was performed as described previously (Kawasaki et al., 2012, 2013; Masuda et al., 2015; Toda et al., 2016). For details, see the Supplemental Experimental Procedures.

DNA Constructs for IUE
pCAG-EGFP was described previously (Wakimoto et al., 2015). pCAG-DN-Cdk5-IRES-EGFP was kindly provided by Dr. Mikio Hoshino and Dr. Takeshi Kawauchi (Kawauchi et al., 2003). DN-Cdk5 was made by replacing Asp at

codon 144 of the Cdk5 protein with Asn (Nikolic et al., 1996). We co-trans-fected 0.5 mg/mL pCAG-EGFP and 3.0 mg/mL DN-Cdk5 into the ferret cere-bral cortex. pX330 plasmid was obtained through Addgene (Mashiko et al., 2013). The pX330-Cdk5 plasmids expressing human Cas9 and sgRNA were prepared by inserting sgRNA oligonucleotides into the BbsI site of pX330. Twenty-nucleotide sequences followed by the protospacer-adjacent motif (PAM) sequence were used as seed sequences for sgRNA. The sgRNA target sequences for Cdk5 are shown in Table S1. If the first nucleotide was not G, we added an extra G at the 5′ end because the U6 promoter prefers a G for tran-scriptional initiation. We transfected pX330-Cdk5-2385 (3.0 or 5.0 mg/mL) or a mixture of three pX330-Cdk5 constructs (pX330-Cdk5-810, pX330-Cdk5-2356, and pX330-Cdk5-2385, 1.67 mg/mL each) with 0.5 mg/mL pCAG-EGFP into the ferret cerebral cortex. Plasmids were purified using the EndoFree plasmid maxi kit (QIAGEN, Germany).

In Situ Hybridization
RNAscope in situ hybridization was performed using RNAscope 2.5 HD detec-tion reagent kit (Advanced Cell Diagnostics) in accordance with the manufac-turer's instructions with modifications. Ferrets were deeply anesthetized and transcardially perfused with 4% paraformaldehyde (PFA) in PBS. Dissected brains were post-fixed overnight with 4% PFA in PBS. To make coronal sections, the brains were cryoprotected by 3-day immersion in 30% sucrose in PBS and embedded in OCT compound. Sections of 16-μm thickness were prepared using a cryostat and pretreated with protease. A Cdk5 probe (GenBank: XM_004765944.2), which was designed by Advanced Cell Diag-nostics, was hybridized with the target Cdk5 RNA. A dapB probe (GenBank: EF191515) targeting the bacterial dapB gene was used as a negative control. The signal was amplified using a multi-step process, followed by hybridization to horseradish peroxidase-labeled probes and chromogenic precipitate devel-opment. The sections were then subjected to Hoechst 33342 staining.

In situ hybridization using digoxigenin-labeled RNA probes was performed as described previously (Kawasaki et al., 2004). Briefly, sections of 16-μm thickness were incubated overnight with digoxigenin-labeled RNA probes in hybridization buffer (50% formamide, 5× saline-sodium citrate buffer, 5× Den-hardt's solution, 0.3 mg/mL yeast RNA, 0.1 mg/mL herring sperm DNA, and 1 mM dithiothreitol). The sections were then incubated with an alkaline phos-phatase-conjugated anti-digoxigenin antibody (Roche) and were visualized using NBT/BCIP as substrates. The sections were then subjected to Hoechst 33342 staining.

We used digoxigenin-labeled RNA probes for ferret Cdk5, Cux1, and Rorb. Cux1 and Rorb probes were kindly provided by Dr. Clifton W. Ragsdale. Two independent ferret Cdk5 cDNA fragments were amplified by RT-PCR and in-serted into the pCRII vector. Two sets of primers (sets 1 and 2) were used to amplify these ferret Cdk5 cDNA fragments. The sequences of the set 1 primers were 5′-GCCGCGATGCAGAAATACAGAG-3′ and 5′-CGAAATACTTCTTA AGGTCCT-3′. The sequences of the set 2 primers were 5′-CTGTGGT ACCGCCCACCGGAT-3′ and 5′-GGGGTTACACTTCAGGAGGTT-3′. The re-sults obtained with the set 1 and the set 2 primers are shown in Figures S1A and S1B, respectively.

Immunohistochemistry
Immunohistochemistry was performed as described previously with modifica-tions (Kawasaki et al., 2000; Toda et al., 2013). For details, see the Supple-mental Experimental Procedures.

Microscopy
Epifluorescence microscopy was performed with a BZ-9000 microscope (KEYENCE, Japan). Confocal microscopy was performed with a FLUOVIEW FV10i (Olympus, Japan) and a LSM 5 PASCAL (Carl Zeiss, Germany).

Next-Generation DNA Sequencing
EGFP-positive regions of the cerebral cortex transfected with pCAG-EGFP and pX330- Cdk5-2385 were dissected under a fluorescent microscope, and genomic DNA was extracted using the DNeasy Blood & Tissue Kit (QIAGEN, Germany). Genomic DNA including the sgRNA target site was PCR-amplified using KOD Plus DNA polymerase (TOYOBO, Japan) with the following primers: 5′-GCAGCTTTCTATCCAGAAGGTGT-3′ (forward) and

5′-TGGGGCAGAATAATGTTTTGGGT-3′ (reverse). The PCR amplicons were subjected to the construction of a library for Illumina sequencing with the KAPA Hyper Prep Kits for Illumina (Kapa Biosystems, Wilmington, MA). In brief, after being purified using AMPure XP beads (Beckman Coulter, Brea, CA), the PCR amplicons were subjected to end repair, A-tailing, adaptor ligation, and PCR amplification for library construction with the KAPA Hyper Prep Kits for Illumina. The library was sequenced using an Illumina MiSeq sequencer (Illu-mina, San Diego, CA) with 2× 300-bp paired-end module. The sequence reads with substantially lower quality (with quality scores <20 on each base) were trimmed with Trimmomatic (Bolger et al., 2014). After trimming, the high-qual-ity sequence reads with a length of at least 200 bp were mapped to the target region of the Mustela putorius furo reference sequence (MusPutFur1.0 scaf-fold00118) using bwa 0.7.12 (Li and Durbin, 2009). CIGAR string in the gener-ated sequence alignment (sam) file was referred to in order to detect sequence reads with deletions from the reference. Sequence reads with deletions were extracted from the bam file, and the reads were reconstructed as fastq files using samtools 1.2 (Li et al., 2009). The deletion-filtered reads were realigned to the reference genome and classified according to the deletion pattern using Sequencher 5.1 (Gene Codes Corp., Ann Arbor, MI). The number of reads in each deletion pattern was counted to determine the frequency of deletions.

Calculation of the Local GS Ratio, the Local GII, and the Local SD Ratio
See the Supplemental Experimental Procedures.

Quantification of Cdk5 Expression
See the Supplemental Experimental Procedures.

Quantification of Glial Markers
See the Supplemental Experimental Procedures.

Quantification of Ki-67, pHH3, Pax6, and Cleaved Caspase 3
See the Supplemental Experimental Procedures.

Statistical Analyses
Statistical analyses were performed using Statcel3 software (OMS Publishing, Japan). To assess statistical significance, p values were determined by the unpaired Welch's t test. "n" means the number of animals.

ACCESSION NUMBERS
The accession number for the next generation sequencing data reported in this paper is DDBJ Sequence Reads Archive: DRA006013.

SUPPLEMENTAL INFORMATION
Supplemental Information includes Supplemental Experimental Procedures, five figures, and one table and can be found with this article online at http://dx.doi.org/10.1016/j.celrep.2017.08.024.

AUTHOR CONTRIBUTIONS
Y.S. and H.K. designed the experiments. Y.S. and Y.T. conducted most of the experiments. T.A.D.D., T.H., and M.K. supported the immunochemical exper-iments. K.H. and A.T. performed sequencing experiments. Y.S. and H.K. wrote the manuscript.

ACKNOWLEDGMENTS

REFERENCES

Barkovich, A.J., Guerrini, R., Kuzniecky, R.I., Jackson, G.D., and Dobyns, W.B. (2012). A developmental and genetic classification for malformations of cortical development: update 2012. Brain *135*, 1348–1369.

Bolger, A.M., Lohse, M., and Usadel, B. (2014). Trimmomatic: a flexible trimmer for Illumina sequence data. Bioinformatics *30*, 2114–2120.

Borrell, V. (2010). In vivo gene delivery to the postnatal ferret cerebral cortex by DNA electroporation. J. Neurosci. Methods *186*, 186–195.

Borrell, V., and Götz, M. (2014). Role of radial glial cells in cerebral cortex folding. Curr. Opin. Neurobiol. *27*, 39–46.

Boycott, K.M., Flavelle, S., Bureau, A., Glass, H.C., Fujiwara, T.M., Wirrell, E., Davey, K., Chudley, A.E., Scott, J.N., McLeod, D.R., and Parboosingh, J.S. (2005). Homozygous deletion of the very low density lipoprotein receptor gene causes autosomal recessive cerebellar hypoplasia with cerebral gyral simplification. Am. J. Hum. Genet. *77*, 477–483.

Cong, L., Ran, F.A., Cox, D., Lin, S., Barretto, R., Habib, N., Hsu, P.D., Wu, X., Jiang, W., Marraffini, L.A., and Zhang, F. (2013). Multiplex genome engineering using CRISPR/Cas systems. Science *339*, 819–823.

Crowley, J.C., and Katz, L.C. (2000). Early development of ocular dominance columns. Science *290*, 1321–1324.

de Juan Romero, C., Bruder, C., Tomasello, U., Sanz-Anquela, J.M., and Borrell, V. (2015). Discrete domains of gene expression in germinal layers distinguish the development of gyrencephaly. EMBO J. *34*, 1859–1874.

DeFelipe, J., Alonso-Nanclares, L., and Arellano, J.I. (2002). Microstructure of the neocortex: comparative aspects. J. Neurocytol. *31*, 299–316.

Fietz, S.A., and Huttner, W.B. (2011). Cortical progenitor expansion, self-renewal and neurogenesis-a polarized perspective. Curr. Opin. Neurobiol. *21*, 23–35.

Fietz, S.A., Kelava, I., Vogt, J., Wilsch-Bräuninger, M., Stenzel, D., Fish, J.L., Corbeil, D., Riehn, A., Distler, W., Nitsch, R., and Huttner, W.B. (2010). OSVZ progenitors of human and ferret neocortex are epithelial-like and expand by integrin signaling. Nat. Neurosci. *13*, 690–699.

Francis, F., Meyer, G., Fallet-Bianco, C., Moreno, S., Kappeler, C., Socorro, A.C., Tuy, F.P., Beldjord, C., and Chelly, J. (2006). Human disorders of cortical development: from past to present. Eur. J. Neurosci. *23*, 877–893.

Fry, A.E., Cushion, T.D., and Pilz, D.T. (2014). The genetics of lissencephaly. Am. J. Med. Genet. C. Semin. Med. Genet. *166C*, 198–210.

Fujishiro, T., Kawasaki, H., Aihara, M., Saeki, T., Ymagishi, R., Atarashi, T., Mayama, C., and Araie, M. (2014). Establishment of an experimental ferret ocular hypertension model for the analysis of central visual pathway damage. Sci. Rep. *4*, 6501.

Gertz, C.C., and Kriegstein, A.R. (2015). Neuronal migration dynamics in the developing ferret cortex. J. Neurosci. *35*, 14307–14315.

Gilmore, E.C., Ohshima, T., Goffinet, A.M., Kulkarni, A.B., and Herrup, K. (1998). Cyclin-dependent kinase 5-deficient mice demonstrate novel developmental arrest in cerebral cortex. J. Neurosci. *18*, 6370–6377.

Guerrini, R., and Marini, C. (2006). Genetic malformations of cortical development. Exp. Brain Res. *173*, 322–333.

Hong, S.E., Shugart, Y.Y., Huang, D.T., Shahwan, S.A., Grant, P.E., Hourihane, J.O., Martin, N.D., and Walsh, C.A. (2000). Autosomal recessive lissencephaly with cerebellar hypoplasia is associated with human RELN mutations. Nat. Genet. *26*, 93–96.

Huberman, A.D., Murray, K.D., Warland, D.K., Feldheim, D.A., and Chapman, B. (2005). Ephrin-As mediate targeting of eye-specific projections to the lateral geniculate nucleus. Nat. Neurosci. *8*, 1013–1021.

Iwai, L., and Kawasaki, H. (2009). Molecular development of the lateral geniculate nucleus in the absence of retinal waves during the time of retinal axon eye-specific segregation. Neuroscience *159*, 1326–1337.

Iwai, L., Ohashi, Y., van der List, D., Usrey, W.M., Miyashita, Y., and Kawasaki, H. (2013). FoxP2 is a parvocellular-specific transcription factor in the visual thalamus of monkeys and ferrets. Cereb. Cortex *23*, 2204–2212.

Johnson, M.B., Wang, P.P., Atabay, K.D., Murphy, E.A., Doan, R.N., Hecht, J.L., and Walsh, C.A. (2015). Single-cell analysis reveals transcriptional heterogeneity of neural progenitors in human cortex. Nat. Neurosci. *18*, 637–646.

Kalebic, N., Taverna, E., Tavano, S., Wong, F.K., Suchold, D., Winkler, S., Huttner, W.B., and Sarov, M. (2016). CRISPR/Cas9-induced disruption of gene expression in mouse embryonic brain and single neural stem cells in vivo. EMBO Rep. *17*, 338–348.

Kawasaki, H., Mizuseki, K., Nishikawa, S., Kaneko, S., Kuwana, Y., Nakanishi, S., Nishikawa, S.I., and Sasai, Y. (2000). Induction of midbrain dopaminergic neurons from ES cells by stromal cell-derived inducing activity. Neuron *28*, 31–40.

Kawasaki, H., Crowley, J.C., Livesey, F.J., and Katz, L.C. (2004). Molecular organization of the ferret visual thalamus. J. Neurosci. *24*, 9962–9970.

Kawasaki, H., Iwai, L., and Tanno, K. (2012). Rapid and efficient genetic manipulation of gyrencephalic carnivores using in utero electroporation. Mol. Brain *5*, 24.

Kawasaki, H., Toda, T., and Tanno, K. (2013). In vivo genetic manipulation of cortical progenitors in gyrencephalic carnivores using in utero electroporation. Biol. Open *2*, 95–100.

Kawauchi, T., Chihama, K., Nabeshima, Y., and Hoshino, M. (2003). The in vivo roles of STEF/Tiam1, Rac1 and JNK in cortical neuronal migration. EMBO J. *22*, 4190–4201.

Kawauchi, T., Chihama, K., Nabeshima, Y., and Hoshino, M. (2006). Cdk5 phosphorylates and stabilizes p27kip1 contributing to actin organization and cortical neuronal migration. Nat. Cell Biol. *8*, 17–26.

Kerjan, G., and Gleeson, J.G. (2007). Genetic mechanisms underlying abnormal neuronal migration in classical lissencephaly. Trends Genet. *23*, 623–630.

Kriegstein, A., and Alvarez-Buylla, A. (2009). The glial nature of embryonic and adult neural stem cells. Annu. Rev. Neurosci. *32*, 149–184.

Kriegstein, A., Noctor, S., and Martínez-Cerdeño, V. (2006). Patterns of neural stem and progenitor cell division may underlie evolutionary cortical expansion. Nat. Rev. Neurosci. *7*, 883–890.

Li, H., and Durbin, R. (2009). Fast and accurate short read alignment with Burrows-Wheeler transform. Bioinformatics *25*, 1754–1760.

Li, H., Handsaker, B., Wysoker, A., Fennell, T., Ruan, J., Homer, N., Marth, G., Abecasis, G., and Durbin, R.; 1000 Genome Project Data Processing Subgroup (2009). The Sequence Alignment/Map format and SAMtools. Bioinformatics *25*, 2078–2079.

Lui, J.H., Hansen, D.V., and Kriegstein, A.R. (2011). Development and evolution of the human neocortex. Cell *146*, 18–36.

Magen, D., Ofir, A., Berger, L., Goldsher, D., Eran, A., Katib, N., Nijem, Y., Vlodavsky, E., Tzur, S., Behar, D.M., et al. (2015). Autosomal recessive lissencephaly with cerebellar hypoplasia is associated with a loss-of-function mutation in CDK5. Hum. Genet. *134*, 305–314.

Martínez-Martínez, M.A., De Juan Romero, C., Fernández, V., Cárdenas, A., Götz, M., and Borrell, V. (2016). A restricted period for formation of outer subventricular zone defined by Cdh1 and Trnp1 levels. Nat. Commun. *7*, 11812.

Mashiko, D., Fujihara, Y., Satouh, Y., Miyata, H., Isotani, A., and Ikawa, M. (2013). Generation of mutant mice by pronuclear injection of circular plasmid expressing Cas9 and single guided RNA. Sci. Rep. *3*, 3355.

Masuda, K., Toda, T., Shinmyo, Y., Ebisu, H., Hoshiba, Y., Wakimoto, M., Ichikawa, Y., and Kawasaki, H. (2015). Pathophysiological analyses of cortical malformation using gyrencephalic mammals. Sci. Rep. *5*, 15370.

Molnár, Z., Métin, C., Stoykova, A., Tarabykin, V., Price, D.J., Francis, F., Meyer, G., Dehay, C., and Kennedy, H. (2006). Comparative aspects of cerebral cortical development. Eur. J. Neurosci. 23, 921–934.

Nikolic, M., Dudek, H., Kwon, Y.T., Ramos, Y.F., and Tsai, L.H. (1996). The cdk5/p35 kinase is essential for neurite outgrowth during neuronal differentiation. Genes Dev. 10, 816–825.

Ohshima, T., Hirasawa, M., Tabata, H., Mutoh, T., Adachi, T., Suzuki, H., Saruta, K., Iwasato, T., Itohara, S., Hashimoto, M., et al. (2007). Cdk5 is required for multipolar-to-bipolar transition during radial neuronal migration and proper dendrite development of pyramidal neurons in the cerebral cortex. Development 134, 2273–2282.

Pilz, D.T., Matsumoto, N., Minnerath, S., Mills, P., Gleeson, J.G., Allen, K.M., Walsh, C.A., Barkovich, A.J., Dobyns, W.B., Ledbetter, D.H., and Ross, M.E. (1998). LIS1 and XLIS (DCX) mutations cause most classical lissencephaly, but different patterns of malformation. Hum. Mol. Genet. 7, 2029–2037.

Poduri, A., Evrony, G.D., Cai, X., and Walsh, C.A. (2013). Somatic mutation, genomic variation, and neurological disease. Science 341, 1237758.

Poluch, S., and Juliano, S.L. (2015). Fine-tuning of neurogenesis is essential for the evolutionary expansion of the cerebral cortex. Cereb. Cortex 25, 346–364.

Pramparo, T., Youn, Y.H., Yingling, J., Hirotsune, S., and Wynshaw-Boris, A. (2010). Novel embryonic neuronal migration and proliferation defects in Dcx mutant mice are exacerbated by Lis1 reduction. J. Neurosci. 30, 3002–3012.

Rakic, P. (1995). A small step for the cell, a giant leap for mankind: a hypothesis of neocortical expansion during evolution. Trends Neurosci. 18, 383–388.

Rakic, P. (2009). Evolution of the neocortex: a perspective from developmental biology. Nat. Rev. Neurosci. 10, 724–735.

Richman, D.P., Stewart, R.M., Hutchinson, J.W., and Caviness, V.S., Jr. (1975). Mechanical model of brain convolutional development. Science 189, 18–21.

Sharma, P., Sharma, M., Amin, N.D., Albers, R.W., and Pant, H.C. (1999). Regulation of cyclin-dependent kinase 5 catalytic activity by phosphorylation. Proc. Natl. Acad. Sci. USA 96, 11156–11160.

Shinmyo, Y., Tanaka, S., Tsunoda, S., Hosomichi, K., Tajima, A., and Kawasaki, H. (2016). CRISPR/Cas9-mediated gene knockout in the mouse brain using in utero electroporation. Sci. Rep. 6, 20611.

Smart, I.H., Dehay, C., Giroud, P., Berland, M., and Kennedy, H. (2002). Unique morphological features of the proliferative zones and postmitotic compartments of the neural epithelium giving rise to striate and extrastriate cortex in the monkey. Cereb. Cortex 12, 37–53.

Sun, T., and Hevner, R.F. (2014). Growth and folding of the mammalian cerebral cortex: from molecules to malformations. Nat. Rev. Neurosci. 15, 217–232.

Sunagawa, G.A., Sumiyama, K., Ukai-Tadenuma, M., Perrin, D., Fujishima, H., Ukai, H., Nishimura, O., Shi, S., Ohno, R., Narumi, R., et al. (2016). Mammalian reverse genetics without crossing reveals Nr3a as a short-sleeper gene. Cell Rep. 14, 662–677.

Toda, T., Homma, D., Tokuoka, H., Hayakawa, I., Sugimoto, Y., Ichinose, H., and Kawasaki, H. (2013). Birth regulates the initiation of sensory map formation through serotonin signaling. Dev. Cell 27, 32–46.

Toda, T., Shinmyo, Y., Dinh Duong, T.A., Masuda, K., and Kawasaki, H. (2016). An essential role of SVZ progenitors in cortical folding in gyrencephalic mammals. Sci. Rep. 6, 29578.

Tsai, L.H., Takahashi, T., Caviness, V.S., Jr., and Harlow, E. (1993). Activity and expression pattern of cyclin-dependent kinase 5 in the embryonic mouse nervous system. Development 119, 1029–1040.

Wakimoto, M., Sehara, K., Ebisu, H., Hoshiba, Y., Tsunoda, S., Ichikawa, Y., and Kawasaki, H. (2015). Classic cadherins mediate selective intracortical circuit formation in the mouse neocortex. Cereb. Cortex 25, 3535–3546.

Walsh, C.A. (1999). Genetic malformations of the human cerebral cortex. Neuron 23, 19–29.

Ware, M.L., Tavazoie, S.F., Reid, C.B., and Walsh, C.A. (1999). Coexistence of widespread clones and large radial clones in early embryonic ferret cortex. Cereb. Cortex 9, 636–645.

White, L.E., Bosking, W.H., Williams, S.M., and Fitzpatrick, D. (1999). Maps of central visual space in ferret V1 and V2 lack matching inputs from the two eyes. J. Neurosci. 19, 7089–7099.

Wynshaw-Boris, A. (2007). Lissencephaly and LIS1: insights into the molecular mechanisms of neuronal migration and development. Clin. Genet. 72, 296–304.

Zecevic, N., Chen, Y., and Filipovic, R. (2005). Contributions of cortical subventricular zone to the development of the human cerebral cortex. J. Comp. Neurol. 491, 109–122.

Zilles, K., Palomero-Gallagher, N., and Amunts, K. (2013). Development of cortical folding during evolution and ontogeny. Trends Neurosci. 36, 275–284.